Journal of Physical and Theoretical Chemistry
of Islamic Azad University of Iran, 18 (3) 37-54: Fall 2021
(J. Phys. Theor. Chem. IAU Iran)
ISSN 1735-2126

Removal Studies of Methyl Orange Dye Using *Ricinus Communis*-capeed Fe_3O_4NPs from Aqueous Solutions

Leila Niknam*, Shahnaz Davoudi

Department of Chemistry, Islamic Azad University, Omidiyeh Branch, Omidiyeh, Iran

Received December 2021; Accepted February 2022

ABSTRACT

The applicability of *Ricinus Communis* functionalized with iron oxide nanoparticles synthesis for eliminating dyes from aqueous media has been confirmed. Identical techniques including FT-IR, BET, XRD and SEM has been utilized to characterize this novel material. The investigation showed the applicability of *Ricinus Communis* functionalized with iron oxide nanoparticles as an available, suitable and low-cost adsorbent for proper deletion of Methyl Orange (MO) dye from aqueous media. The pH value of 5.0, adsorbent dosage of 0.3 g, (MO) dye concentration of 50 mg/L, and contact time of 60 min have been considered the optimum values of adsorption onto *Ricinus Communis*-capeed Fe_3O_4NPs. Studying the impact of different parameters revealed that the adsorption percentage and the initial (MO) dye concentration have been inversely related while the adsorption percentage and adsorbent dosage have been directly related. It was shown that the adsorption of (MO) dye deletion by adsorbent was at pH 5.0. The Langmuir model got better of other models in describing the equilibrium data. Thermodynamic parameters of free energy (ΔG^0), enthalpy (ΔH^0) and entropy (ΔS^0) of adsorption were determined using isotherms. The fact that the sorption process was exothermic was well reflected by the negative value of (ΔG^o, ΔH^o and ΔS^o) which on its own expressed the affinity of *Ricinus Communis*-capeed Fe_3O_4NPs for deleting (MO) dye. The maximum adsorption capacity (q_{max}) was observed to be (30.5 mg g^{-1}) for (MO) dye at desired conditions.

Keywords: Methyl Orange (MO) dye, Adsorption capacity, Langmuir isotherms, Thermodynamic

1. INTRODUCTION

Industrial effluents contain dyes with large amounts of suspended organic solids [1]. Presence of such effluents in water could generate hazards to aquatic life by enhancing mutagenic and carcinogenic effects. Textile, paper, and printing activities are some sources of dye-containing wastewater [2,3].

*Corresponding author: leila.niknam352@gmail.com

Dyes and pigments have been extensively released in the wastewaters from different industries, particularly from textile, paper, rubber, plastic, leather, cosmetic, food, and drug industries. These dyes can cause allergic dermatitis, skin irritation, cancer and mutation in living organisms. It also causes eye burns, which may be responsible for permanent injury to the eyes of human and animals. On inhalation, it can give rise to short periods of rapid or difficult breathing, while ingestion through the mouth produces a burning sensation and may cause nausea, vomiting, profuse sweating, mental confusion, painful micturation, and methemoglobinemia–like syndromes [4,5]. Because of their synthetic natures and complex aromatic molecular structures, dyes are almost non-biodegradable in the ecosystem. The importance of the potential pollution of dyes and their intermediates has been incited with the toxic nature of many dyes, different mutagenic effects, skin diseases and skin irritation and allergies. Moreover, they are dangerous because their microbial degradation compounds, such as benzidine or other aromatic compounds have carcinogenic effect [6].

Azo dyes are divided according to the presence of azo bonds (–N=N–) in the molecule; these include mono azo, diazo, triazoetc [7]. Azo dyes resist the effect of oxidation agents and light, thus they cannot be completely treated by conventional methods of anaerobic digestion. It is necessary to find an effective method for the treatment of Methyl Orange (MO) dye (Fig. 1). The degradation of Methyl Orange (MO) dye in the presence of aqueous iron oxide suspension has been reported before [8]. It shows several side effects such as eye and skin sensitivity. Also, inhalation of its dust may cause digestion and respiratory tract irritation. (Fig. 1), is a hazardous dye that is widely used for dyeing of wool and silk, carbon paper, cosmetics, and leather [9].

Adsorption is one of the best and simple techniques for the removal of toxic and noxious impurities in comparison to other conventional protocols like chemical coagulation, ion exchange, electrolysis, biological treatments is related to advantages viz. lower waste, higher efficiency and simple and mild operational conditions. Adsorption techniques also have more efficiency in the removal of pollutants which are highly stable in biological degradation process through economically feasible mild pathways [10-12]. The best figures of merit in multi component dyes systems removal are based on development of novel method that permits their accurate simultaneous determination in mixtures. The encounter difficulties are serious peaks overlapping that subsequently impossible their direct determination in mixture using general equation like Beer–Lambert. Derivative spectroscopy efficiently is applicable to resolve absorption peaks overlap through their separation and correction of background interferences. This method is based on searching the wavelengths that possible the accurate and repeatable monitoring of each species in complex matrices without any interference from other target compounds [13,14]. Hence, it has been extensively used for removal of different chemicals from aqueous solutions [15,16]. Of these methods, nanomaterial's based adsorbents is highly recommended for dyes pollutants removal [17]. The efficient applicability of an adsorption process mainly depends on the physical and chemical characteristics of the adsorbent, which is expected to have high adsorption capacity and to be recoverable and available at economical cost. Currently, various potential adsorbents have been implemented for removal of specific organics from water samples. In

this regard, magnetic nanoparticles (MNPs) have been studied extensively as novel adsorbents with large surface area, high adsorption capacity and small diffusion resistance. For instance, they have been used for separation of chemical species such as environmental pollutants, metals, dyes, and gases [18,19].

In this current study, after synthesizing *Ricinus Communis*-capeed Fe_3O_4NPs as a unique adsorbent, its characterization by Fourier transform infrared spectroscopy (FTIR), scanning electron microscopy (SEM), and X-ray diffraction (XRD) analysis has been carried out. In the process of Methyl Orange (MO) dye deletion, the effects of important variables like contact time, pH of solution, adsorbent dosage and (MO) dye concentration as well as the dye deletion percentage as response were investigated and optimized. The fact that the pseudo-second-order rate equation matched the adsorption of (MO) dye was evident. Also the Langmuir model could get better of other models in explaining the equilibrium data. However specific isotherm models viz, Freundlich, Langmuir, and Tempkin were used to fit the experimental equilibrium data. But eventually the findings confirmed the suitability and applicability of the Langmuir model. Moreover, it was shown that the kinetic of adsorption process between the kinetic models of pseudo-first-order and pseudo-second-order diffusion models was under the control of the latter one. The success of the *Ricinus Communis*-capeed Fe_3O_4NPs in deleting the dyes effectively was proven.

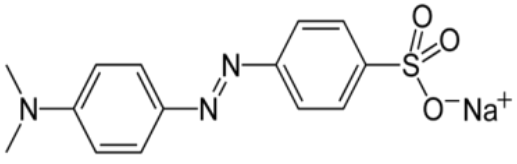

Figure 1: Chemical structure of Methyl Orange (MO) dye.

2. EXPERIMENTAL

2.1. Reagents and instruments

Methyl Orange (MO) dye (99%), sodium hydroxide (99%), hydrochloric acid (37%), Iron Oxide (%). They were supplied from Merck (Darmstadt, Germany). The morphology of samples was studied by scanning electron microscopy (SEM: KYKY-EM 3200, Hitachi Company, China) under an acceleration voltage of 26kV). The pH/Ion meter (model-728, Metrohm Company, Switzerland, Swiss) was used for the pH measurements. Dyes concentrations were determined using Jasco UV–Vis spectrophotometer model V-530 (Jasco Company, Japan).

2.2. Preparation of Biomass.

The *Ricinus Communis* powder was collected this material is a zero-value agricultural waste product. *Ricinus Communis* was plucked off the woody parts of the *Ricinus Communis* powder plant, thoroughly washed with water, and sun dried for 5 days. The dried biomass was milled and then fractionated using 100 - 300 m analytical sieves and washed twice with 0.01 M HCl in order to remove any dyes that might be on the biomass.

2.3. Preparation Ricinus Communis-capeed Fe_3O_4 NPs

Fe_3O_4NPs were prepared by mixing $FeCl_2{\cdot}4H_2O$ (2.74 g), $FeCl_3{\cdot}6H_2O$ (3.11 g) and 0.85 mL concentrated hydrochloric acid into 25 mL deionized water. The mixture was added to a stirred 250 mL NaOH solution (1.5 M). In the designed method, the synthesis of Fe_3O_4NPs was done by introducing nitrogen gas through a sparer into the solution for oxygen removal. The bubbling of nitrogen gas through the solution protects Fe_3O_4 against critical oxidation and reduces the particles size when compared to synthesis methods without oxygen removal [20].

During the whole process, the solution temperature was maintained at 80°C. After completion of the reaction, the obtained Fe_3O_4NPs were separated from the reaction medium by the magnetic field, then we increased the bath temperature to 90°C. The sediment suspension was stirred for 3 hours. Stirring was stopped and the suspension was placed in the laboratory for 2 hours. The carbon-produced suspensions were prepared from a leaf medlar with an equal weight ratio and after analysis, BET, XRD, FT-IR and SEM were used as adsorbent.

2.4. Batch adsorption dyes adsorption process

To ascertain the (MO) dye adsorption isotherm onto *Ricinus Communis*-capeed Fe_3O_4NPs and also to determine its kinetic properties, batch adsorption tests were executed. First, 250 mL solution containing 50 mg/L concentration of (MO) dye was provided. When adjustment of initial pH of the solution was done by 0.01N HCl / 0.01N NaOH aqueous solution, no further adjustments were performed in the course of the trials. By dividing this 250 mL solution into ten samples of 50 mL, ten flasks (50 mL) with fixed adsorbent dose of 50 mg/L were provided. With the help of an orbital shaker, these flasks were agitated at a steady rate of 180 rpm and controlled temperature of 25^{oC}. At fixed time intervals, one flask was withdrawn from orbital shaker (30, 40, 50, 60, 80 at 90 min) and the analysis of the remaining (MO) dye in the sorbate solution was performed. The (MO) dye concentration in the solution was measured using a double beam UV–vis spectrophotometer (jasco, Model UV–vis V-530, Japan) set at wavelengths 650 nm for (MO) dye. The amount of adsorbed dye at equilibrium (qe(mg/g)) was calculated using equation:

$$0/0dye = \frac{(C_\circ - C_t)}{C_\circ} \times 100 \quad (1)$$

Where $C_\circ(mgL^{-1})$ C_0 $(mg\ L^{-1})$ refers to the concentration of target at initial time t and $C_t(mgL^{-1})$ C_t $(mg\ L^{-1})$ stands for the concentration of target after time t.

$$q_e = \frac{(C_\circ - C_e)V}{W} \quad (2)$$

In the above equation Q refers to the quantity of dyes adsorbed onto unit quantity of sorbent (mg g^{-1}); C_0 demonstrates the concentrations (mg mL^{-1}) of dyes in the primary solution and the concentrations of dyes in the aqueous phase after adsorption is demonstrated by C. The volume of the aqueous phase (mL) is shown by V; and w shows the weight of the sorbent (g). In addition, the effect of three critical parameters of pH, concentrations, and contact time were investigated in the present work [21,22].

3. RESULTS AND DISCUSSION

3.1. Characterization of adsorbent

3.1.1. BET analysis of Ricinus Communis-capeed Fe_3O_4 NPs

The pore structure parameters of molecular sieve materials such as N_2 adsorption-desorption isothermal curve and specific surface area were determined by micrometrics adsorption analyzer. The sample was dropped onto the slide for conducting layer treatment, at 77 K liquid nitrogen temperature and the operating voltage was 20 KV. The specific surface area was calculated using the Brunner-Emmett-Teller (BET) method. The bulk density affects the rate of adsorption of (MO) dye solution onto *Ricinus Communis*-capeed Fe_3O_4NPs shown in Table 1. In the present study, the bulk density was less than 2.0 indicating that the activated carbon materials are in fine nature and hence enhanced the adsorption

of (MO) dye solution from aqueous solution. The moisture content (0.3%) was determined, even though it does not affect the adsorption power, dilutes the adsorbents, and therefore necessitates the use of additional weight of adsorbents to provide the required weight [23]. The surface area of *Ricinus Communis*-capeed Fe_3O_4NPs in the present research study was (45.231 m^2/g and 1.34×10^{-2} cm^3/g).

3.1.2. FTIR analysis

FTIR spectra for *Ricinus Communis*-capeed Fe_3O_4NPs are shown in (Fig. 2). The vibrational frequencies for stretching bonds in PSF membrane molecule cannot be detected by FTIR analysis. This confirms that *Ricinus Communis*-capeed Fe_3O_4NPs doesn't show any definite absorption peaks in the range 400 - 4000 cm^{-1}. The vibration modes located at 3451 cm^{-1} can be assigned to the O–H broad absorption mode due to the hydroxyl group in the compound. The absorption band at 1558 cm^{-1} is due to the O–H bending vibration from the water molecules adsorbed into the surface. The absorption band at 745 and 545 cm^{-1} is due to the Fe–O bending in the molecules adsorbed into the surface. There is a furthermore subtle point that no significant difference between the FTIR spectra of *Ricinus Communis*-capeed Fe_3O_4NPs is observed [24].

3.1.3. XRD analysis

The XRD pattern of the *Ricinus Communis*-capeed Fe_3O_4NPs (Fig. 3), represents show peaks at 2θ= 30.2°, 36.5°, 38.8°, 53.2°, 60.4° and 62.4° belong to the lattice planes of (222), (311), (422), (400), (511) and (440), confirm the cubic structure of *Ricinus Communis*-capeed Fe_3O_4NPs [25]. As can be seen, the entirely crystalline structure is confirmed, while the high intensity of peak at 38.8° (311) indicates the presence of a low quantities of substances in an amorphous condition.

Table 1: Characteristics of the *Ricinus Communis*-capeed Fe_3O_4 NPs

Parameter	pH	Bulk density (g/mL)	Surface area (m^2/g)	Particle size range (µm)	Loss of mass on ignition
Value	7.0	0.607	250.0	45.0-250.0	0.6235

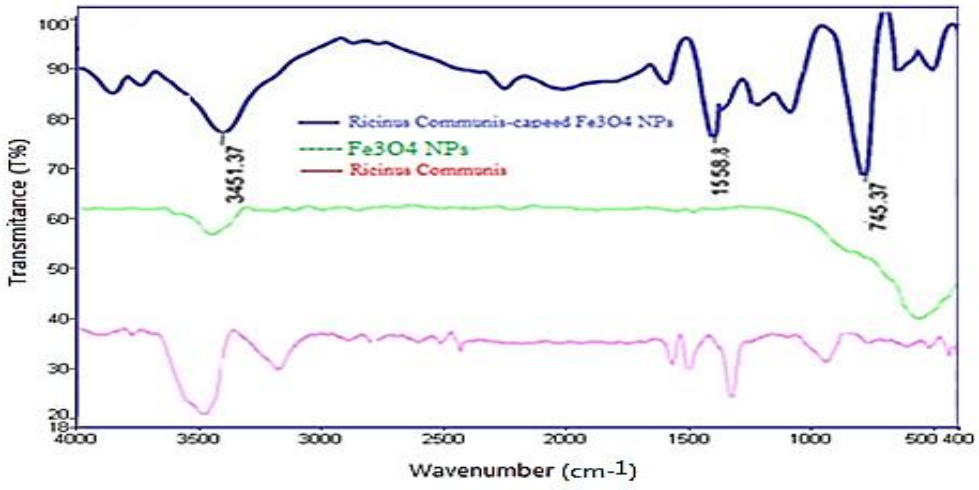

Figure 2: FT-IR transmittance spectrum of the prepared *Ricinus Communis*-capeed Fe_3O_4 NPs.

3.1.4. Surface morphology

The morphological properties of *Ricinus Communis*-capeed Fe_3O_4 NPs was investigated by FE-SEM and is exhibited in (Fig. 4), the evenness, homogeneity, orderliness and approximate uniformity of synthesized *Ricinus Communis*-capeed Fe_3O_4 NPs (even in size distribution) can be observed. *Ricinus Communis*-capeed Fe_3O_4 NPs after surface modification came to be uneven, bigger and agglomerate**.** It can be seen that the particles are mostly spherical with the various size distribution as they form agglomerates. Based on the particle size distribution, we obtained the average particle size in the range of 40-60 nm very close to those determined by XRD analysis [25].

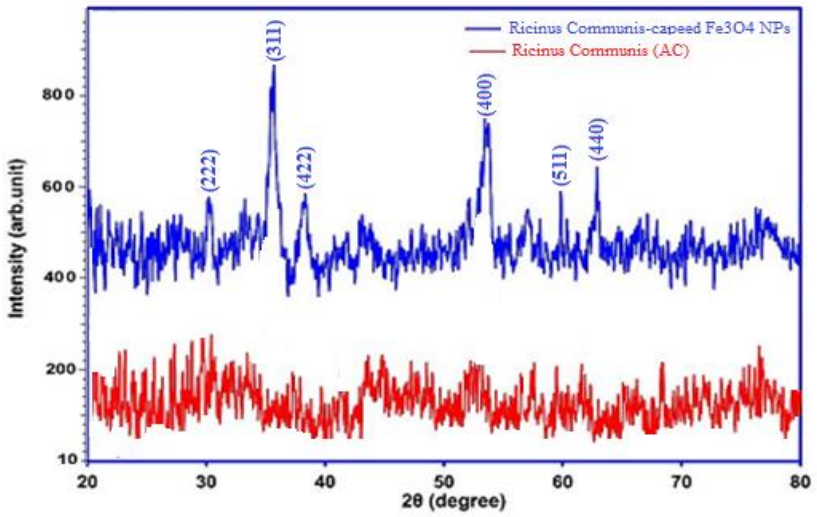

Figure. 3: X-ray diffraction of *Ricinus Communis*-capeed Fe_3O_4 NPs.

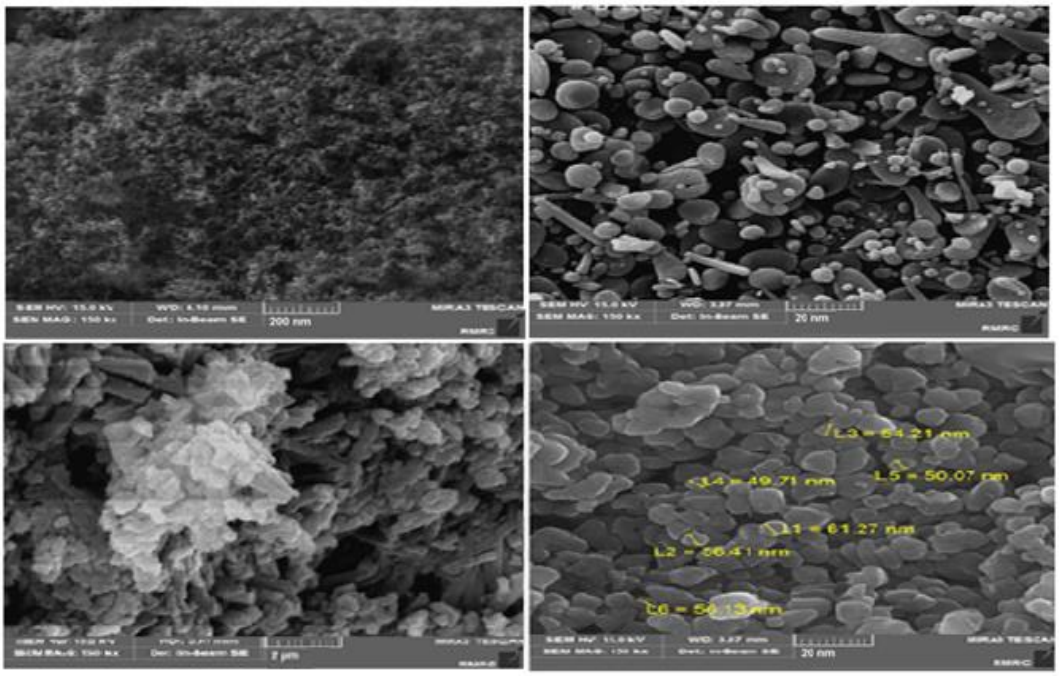

Figure. 4: The (SEM) image of the prepared *Ricinus Communis*-capeed Fe_3O_4 NPs.

3.2. Impact of pH on the adsorption

The pH has been identified as one of the most important parameter that is effective on dyes sorption. The effect of pH on the (MO) dye onto *Ricinus Communis*-capeed Fe_3O_4NPs was studied at pH4.0–9.0, shown in (Fig. 5). The maximum sorption was observed at pH 5.0 for (MO) dye. The remaining all sorption experiments were carried out at this pH value. The sorption mechanisms on the *Ricinus Communis*-capeed Fe_3O_4NPs of the physic chemical interaction of the solution [27, 28]. At highly acidic pH, the overall surface charge on the active sites became. The positive and (MO) dye and protons compete for binding sites on *Ricinus Communis*-capeed Fe_3O_4NPs. Which results in lower uptake of (MO) dye. The sorbent surface was more negatively charged as the pH solution increased from pH 5.0 for (MO) dye. The functional groups of the *Ricinus Communis*-capeed Fe_3O_4NPs was more deprotonated and thus available for the (MO) dye. Decrease in sorption yield at higher pH 5.0 for the (MO) dye is not only related to the formation of soluble hydroxylated complexes of the (MO) dye, but also to the ionized nature of the *Ricinus Communis*-capeed Fe_3O_4NPs of the sorbent under the studied pH. Previous studies also reported that the maximum sorption efficiency of (MO) dye on biomass was observed at pH (5.0).

3.3. Impact of the dosage of sorbent

The sorbent dosage is an important parameter because this determines the capacity of a sorbent for a given initial concentration. The sorption efficiency for (MO) dye as a function of sorbent dosage was investigated. The percentage of the metal sorption steeply increases with the sorbent loading up to 0.3 g in (Fig. 6). This result can be explained by the fact that the sorption sites remain unsaturated during the sorption reaction, whereas the number of sites available for sorption site increases by increasing the sorbent dose [29]. The maximum sorption was attained at sorbent dosage, 0.3 g. Therefore, the optimum sorbent dosage was taken as 0.3 g for further experiments. This can be explained by when the sorbent ratio is small, the active sites for binding dye on the surface of *Ricinus Communis*-capeed Fe_3O_4NPs is less, so the sorption efficiency is low. As the sorbent dose increased, more active sites to bind (MO) dye, thus it results an increase in the sorption efficiency until saturation [30].

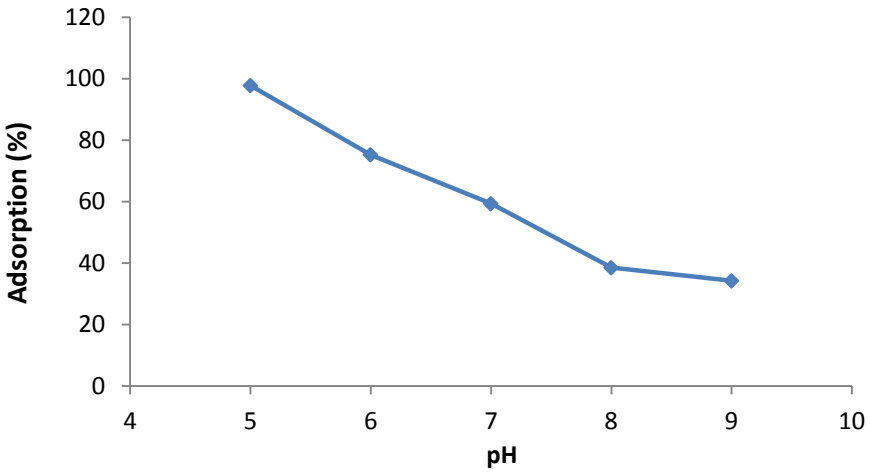

Figure 5: impact of initial solution pH on the adsorption amount of (MO) dye onto *Ricinus Communis*-capeed Fe_3O_4NPs. [(MO) dye = 50.0 mgL^{-1}; dosage sorbent = 0.3 g; time = 60.0 min; stirring speed = 180 rpm].

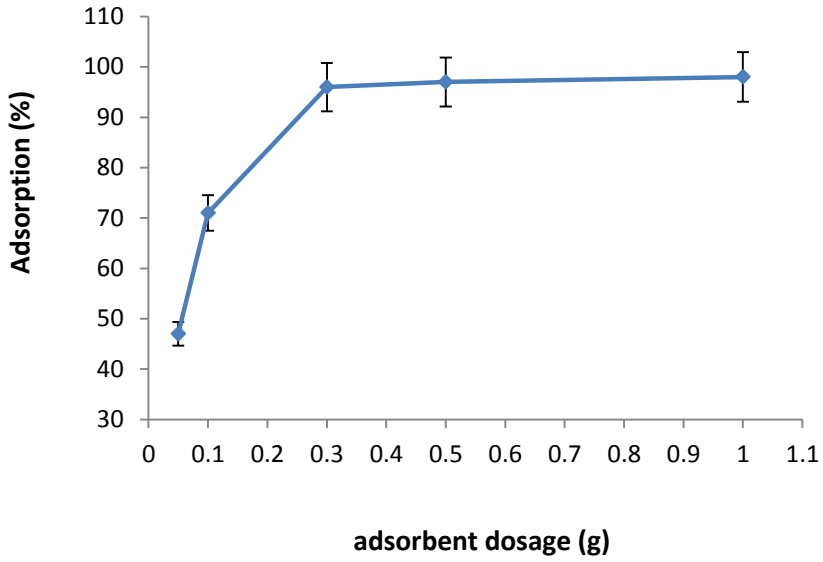

Figure. 6: Impact of dosage sorbent on the adsorption amount of (MO) dye. [(MO) dye = 50.0 mgL^{-1}; pH =5.0; time = 60.0 min; stirring speed = 180 rpm].

3.4. Impact of the contact time on the adsorption

Since the rate of sorption is considered crucial for designing batch bio sorption experiments, thus, the impact of contact time on the sorption of (MO) dye by *Ricinus Communis*-capeed Fe_3O_4NPs was examined. A considerable increase in the sorption of (MO) dye was observed for the contact time of 60 min. The impact of initial dye concentration (MO) dye sorption by a *Ricinus Communis*-capeed Fe_3O_4NPs was scrutinized in batch experiments applying 30 at 90 min contact time, pH value 5 for Methyl Orange (MO) dye, 0.3 g adsorbent dose and the constant temperature 300.15 K [31,32]. With an increase in the initial concentration of (MO) dye, a gradual boost in the equilibrium uptake of the sorbent was observed. The elevation of sorption yield along with the elevation in dye concentration can probably be a result of higher interaction between the (MO) dye and sequestering sites of the sorbent shown in (Fig. 7).

3.5. Impact of the temperature

To study the effects of temperature on the adsorption of (MO) dye by *Ricinus Communis*-capeed Fe_3O_4NPs, the experiments were performed at temperatures from 298.15 to 328.15 K. Fig. 8, shows the influence of temperature on the adsorption of dye on *Ricinus Communis*-capeed Fe_3O_4NPs. As it was observed, the equilibrium adsorption capacity of (MO) dye onto *Ricinus Communis*-capeed Fe_3O_4NPs was found to increase with increasing temperature. This fact indicates that the mobility of dye molecules increased with the temperature, additionally the viscosity of dye solution reduces with rise in temperature and as a result, it increases the rate of diffusion of dye molecules. The results were in agreement with the effect of the solution pH, and temperature on adsorption behavior of reactive (MO) dye on *Ricinus Communis*-capeed Fe_3O_4NPs [33,34].

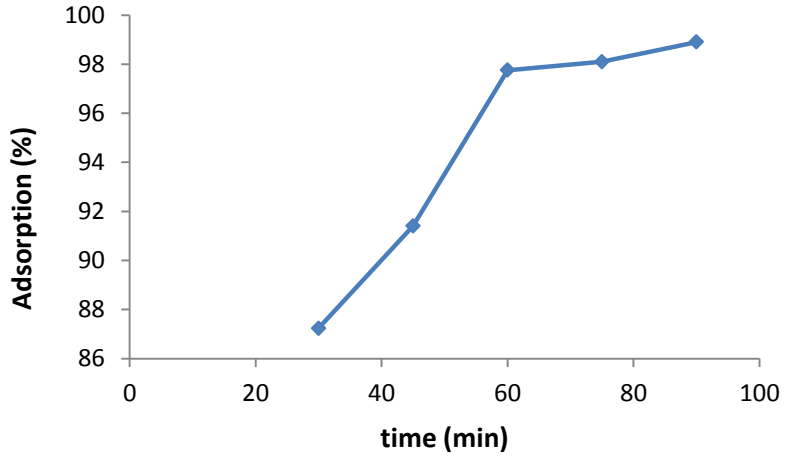

Figure 7: Impact of contact time on the adsorption of (MO) dye by *Ricinus Communis*-capeed Fe_3O_4NPs [(MO) dye = 50.0 mgL^{-1}; pH =5.0; dosage sorbent = 0.3 g; stirring speed = 180 rpm].

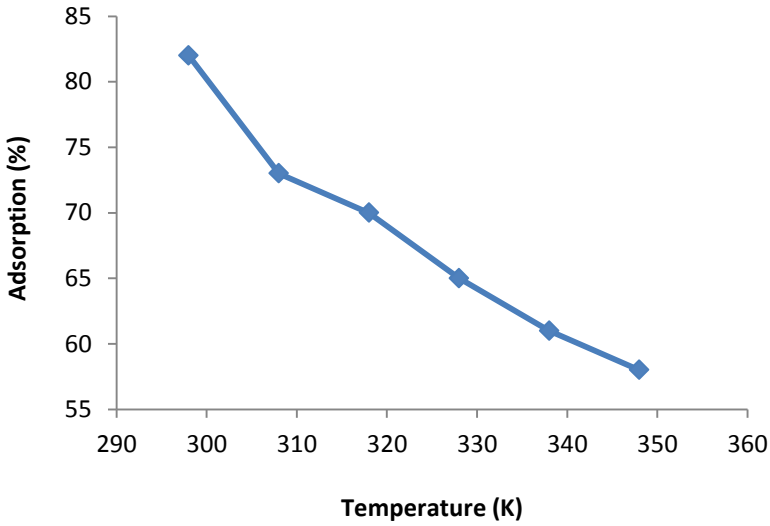

Figure 8: Impact of temperature on the adsorption amount of (MO) dye onto *Ricinus Communis*-capeed Fe_3O_4NPs [(MO) dye = 50.0 mgL^{-1}; pH =5.0; dosage sorbent = 0.3 g; time = 60.0 min; stirring speed = 180 rpm].

3.7. Adsorption equilibrium survey

The equilibrium relationship premised on mathematical connection of an established equilibrium between the amount of adsorbed target per gram of adsorbent (q_e(mg/g)) to the equilibrium non-adsorbed quantity of dyes in solution (C_e (mg/L) at specified temperature is defined by adsorption equilibrium isotherms [35,36]. Under the auspices of 3 models of Langmuir, Freundlich and Temkin isotherms, the adsorption isotherm of adsorption was scrutinized.

1) Based on Langmuir adsorption isotherm model: no interaction existed amongst adsorbed molecules and adsorption process on uniform surfaces. The ensuing equation presents Langmuir model [37]:

$$C_e/q_e = 1/K_L q_{max} + C_e/q_{max} \quad (3)$$

In the foregoing equation, the equilibrium concentration, the adsorption capacity and the maximum adsorption capacity of the adsorbents in the aqueous medium are shown by C_e (mg/L), q_e

(mg/g) and q_{max}(mg/g) respectively. K_L as a constant is associated with binding energy of the sorption system (L/mg) (Fig. 9a).

2) Freundlich adsorption isotherm: This model can be explained the multilayer adsorption of an adsorbate onto a heterogeneous surface of an adsorbent. The linear form of Freundlich isotherm model expression is given as:

$$\ln q_e = \ln K_F + \frac{1}{n} \ln C_e \quad (4)$$

That K_f (the adsorption capacity) and n (intensity of a given adsorbent) are the Freundlich isotherm constant (Fig. 9b).

The values of the constants in both models are obtained from the slope and the position (Fig. 9b). Table 1: shows the results of the fit and of the constants of both models for (MO) dye. The values of n for (MO) dye onto activated carbon derived from Corn Husk functionalized with iron oxide nanoparticles. The values between 1 and 10 for n in the adsorption process are favorable [38]. All the correlation coefficients and parameters obtained for the isotherm models from (Table 2) reveal that the Langmuir isotherm is the best model to demonstrate the adsorption of (MO) dye onto *Ricinus Communis*-capeed Fe_3O_4NPs adsorbent.

3) In Temkin isotherm equation, there exists a presumption that the heat of sorption of all the molecules in the layer reduces linearly with coverage owing to adsorbent–adsorbate interactions And also it is presumed that the adsorption is characterized by a uniform distribution of the binding energies up to some top binding energy [39]. The ensuing introduces the linear form of the Temkin isotherm:

$$q_e = \frac{Rt}{b} ln\, K_T + \frac{RT}{b} ln C_e \quad (5)$$

In Fig. 9c, the plots of ln (C_e) versus q_e for (MO) dye are exhibited and in (Table.1), the linear isotherm parameters b_T, K_T and the correlation coefficient are summarized. The b_T constant relative to heat of sorption for (MO) dye onto *Ricinus Communis*-capeed Fe_3O_4NPs adsorbent equals 21.441 J/mol.

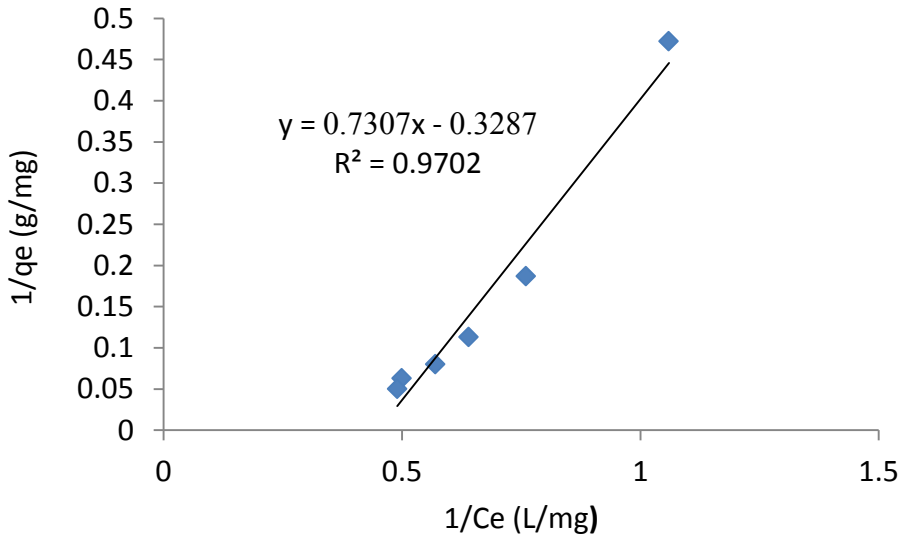

Figure. 9a: Langmuir isotherm for the adsorption of (MO) dye [(MO) dye = 50.0 mgL^{-1}; pH =5.0; dosage sorbent = 0.3 g; time = 60.0 min; stirring speed = 180 rpm].

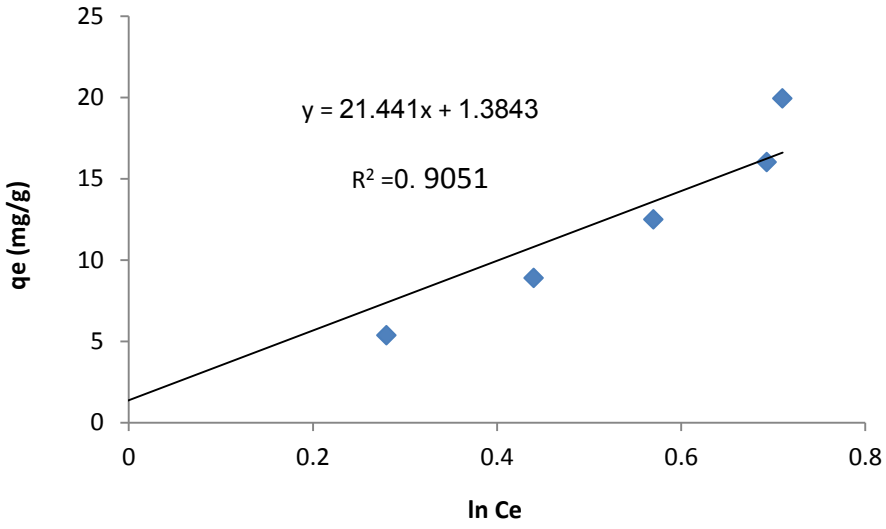

Figure 9b: Freundich isotherm for the adsorption of (MO) dye [(MO) dye = 50.0 mgL^{-1}; pH =5.0; dosage sorbent = 0.3 g; time = 60.0 min; stirring speed = 180 rpm].

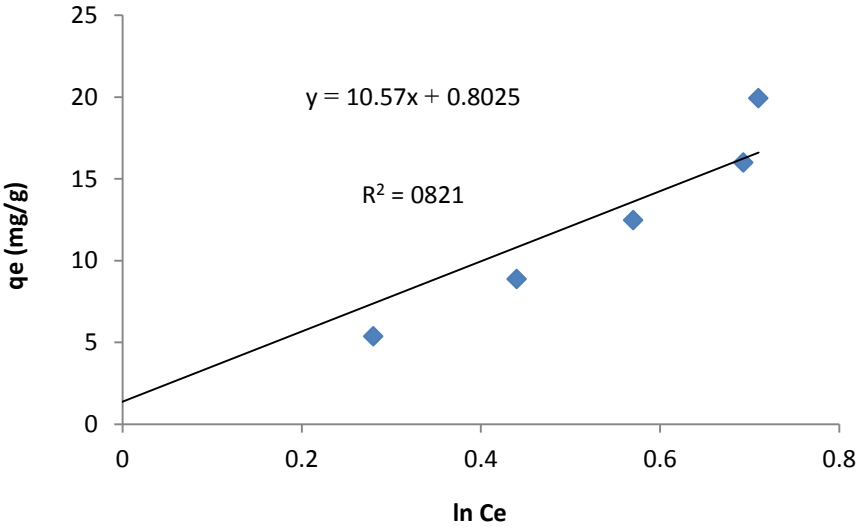

Figure 9c: Temkin isotherm for the adsorption of (MO) dye [(MO) dye = 50.0 mgL^{-1}; pH =5.0; dosage sorbent = 0.3 g; time = 60.0 min; stirring speed = 180 rpm].

Table 2: Various isotherm constants and correlation coefficients calculated for the adsorption of dye onto *Ricinus communis*-capeed Fe_3O_4NPs. [(MO) dye = 50.0 mgL^{-1}; pH =5.0; dosage sorbent = 0.3 g; time = 60.0 min; stirring speed = 180 rpm].

Isotherms	**(MO) dye**		
Langmuir	q_{max}	K_a(L/mg)	R^2
	30.5	0.46	0.9702
Freundich	K_F $(mg)^{1-n}$ $L^n g^{-1}$	n(g/L)	R^2
	12.7	0.39	0.9051
Temkin	B_T	K_T (L mg^{-1})	R^2
	21.5	1.06	0.821

3.8. The adsorption kinetic surveys

Adsorption of a solute by a solid in aqueous solution through complex stages, is strongly influenced by several parameters related to the state of the solid (generally with very heterogeneous reactive surface) and to physico- chemical conditions under which the adsorption occurred. The rate of dyes adsorption onto adsorbent was fitted to traditional models like, pseudo-first and pseudo- second-models [40,41]. The Lagergren pseudo-first order modeled scribed the adsorption kinetic data [42]. The Lagergren is commonly expressed as follows:

$$\frac{dq_t}{dt}=k_1(q_e-q_t) \quad (6)$$

Where q_e an dq_t(mg/g) are the adsorption capacities at equilibrium and at time t, respectively. k_1 is the rate constant of the pseudo-first-order adsorption(L/min). The log (q_e-q_t) versus t was plotted and the values of k_1 and q_e were determined by using the slope and intercept of the line, respectively.

$$\log(q_e-q_t)=\log q_t-(\frac{k_1}{2.303})t \quad (7)$$

The fact that the intercept is not equal to q_e implies that there action is unlikely to follow the first-order. The relation ship between initial solute concentration and rate of adsorption is linear when pore diffusion limits the adsorption process. Therefore, it is necessary to fit experimental data to another model (Table. 3) such as pseudo-second order model [43], based on the following equation:

$$\frac{dq_t}{dt}=k_2(q_e-q_t)^2 \quad (8)$$

Eq.(7) is integrated over the interval 0 to t for t and 0 to $q_t$for q_t, to give

$$\frac{t}{q_t}=\frac{1}{k_2q_e^2}+\frac{t}{q_e} \quad (9)$$

As mentioned above, the plot of log (q_e-q_t) versus t does not show good results for entire sorption period, while the plot of t/q_t versus t shows a straight line. The values of k_2 and equilibrium adsorption capacity (q_e) were calculated from the intercept and slope of the plot of t/q versus t (Table. 3). The calculated q_e values at different working conditions like various initial dyes concentrations and/or adsorbent masses were close to the experimental data and higher R^2 values corresponding to this model confirm its more suitability for the explanation of experimental data [42,43]. This indicates that the pseudo-second-order kinetic model applies better for the adsorption of (MO) dye system for the entire sorption period. The kinetic data from pseudo-first and pseudo-second-order adsorption kinetic models given in (Table. 3). The linear plots of t/q_t versus t indicated a good agreement between the experimental and calculated $q_e$values for different initial dyes concentrations. Further more, the correlation coefficients of the pseudo-second-order kinetic model ($R^2 = 0.9814$) were greater than that of the pseudo-first-order model (R^2= 0.8331) for (MO) dye respectively. As a result, respectively. As a result, the adsorption fits to the pseudo-second-order better than the pseudo-first-order kinetic model.

3.9. Adsorption thermodynamics

For the adsorption processes, 3 thermodynamic parameters of 1-Gibbs free energy change (ΔG°), 2- enthalpy change (ΔH°) and 3- entropy change ΔS° were considered. Their computation becomes possible through utilizing the ensuing equations [44]:

$$\Delta G^\circ = -RT\ln K_{ad} \quad (10)$$

$$\ln K_{ad}\frac{\Delta H^\circ}{RT}+\frac{\Delta S^\circ}{R} \quad (11)$$

From a plot of lnKe against 1/T, a graph (Fig. 12) is provided. By considering the

slope of this graph ΔG can be acquired. In Table. 5, the summary of the thermodynamic parameter outcomes for the adsorption of (MO) dye onto *Ricinus Communis*-capeed Fe_3O_4NPs at diverse temperatures is demonstrated.

The estimation of ΔG^o values became possible via employing the equation adsorption of (MO) dye. As can be seen in (Fig. 12), with any increase in the temperature from 300.15 to 353.15 K, a steep reduction in the *Ricinus Communis*-capeed Fe_3O_4NPs adsorbent was observed which confirms the exothermicity nature of the process. The values of the thermodynamic parameters (Table. 5). were computed using the plots. The feasiability and spontaneity nature of the process was revealed by the negative value of ΔG^o. On the other hand, the exothermicity nature of adsorption was proven by the negative value of ΔH^o and the value of ΔS^o was a good indication of change in the randomness at the *Ricinus Communis*-capeed Fe_3O_4NPs solution interface during the sorption. The fact that ΔG^o values up to -4.7 J/mol (MO) dye are accordant with electrostatic interaction between sorption sites and the (MO) dye (physical adsorption) has been reported. The obtained ΔG^o values in this article for (MO) dye are <-5 J/mol suggesting the predominancy of the physical adsorption mechanism in the sorption process [45,46].

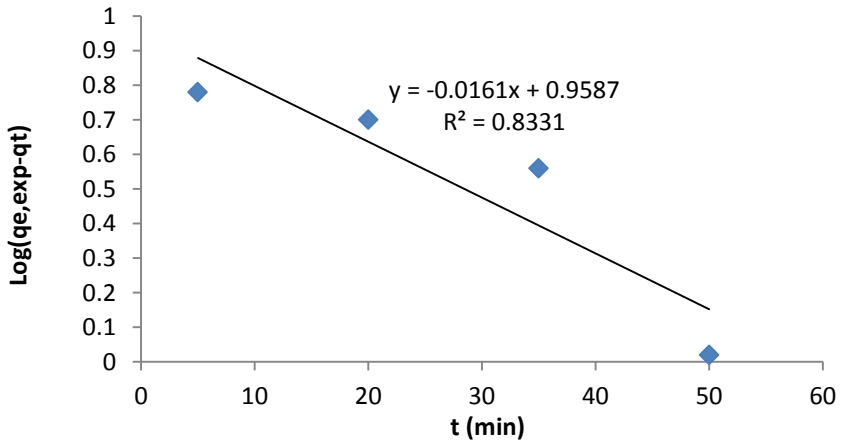

Figure 10: Pseudo-first-order kinetics for (MO) dye onto *Ricinus Communis*-capeed Fe_3O_4NPs. [(MO) dye = 50.0 mgL^{-1}; pH =5.0; dosage sorbent = 0.3 g; time = 60.0 min; stirring speed = 180 rpm].

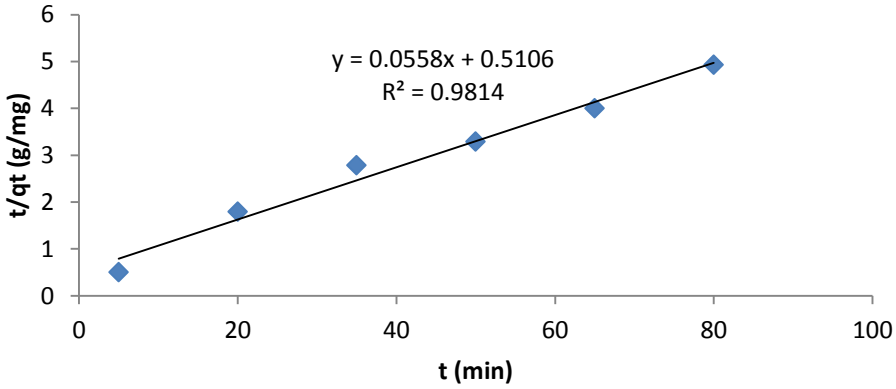

Figure 11: Pseudo-second-order kinetics for (MO) dye onto *Ricinus Communis*-capeed Fe_3O_4NPs. [(MO) dye = 50.0 mgL^{-1}; pH =5.0; dosage sorbent = 0.3 g; time = 60.0 min; stirring speed = 180 rpm].

Table 4: Kinetic parameters for the adsorption of dye onto *Ricinus Communis*-capeed Fe_3O_4NPs. [(MO) dye = 50.0 mgL^{-1}; pH =5.0; dosage sorbent = 0.3 g; time = 60.0 min; stirring speed = 180 rpm]

Kinetic Model	Pseudo first - order kinetic			seudo second-order kinetic		
	q_e(mg g^{-1})	K_1(1/min)	R^2	q_e(mg g^{-1})	K_2(g/mg min)	R^2
(MO) dye	9.1	0.04	0.8331	18.0	6.1	0.9814

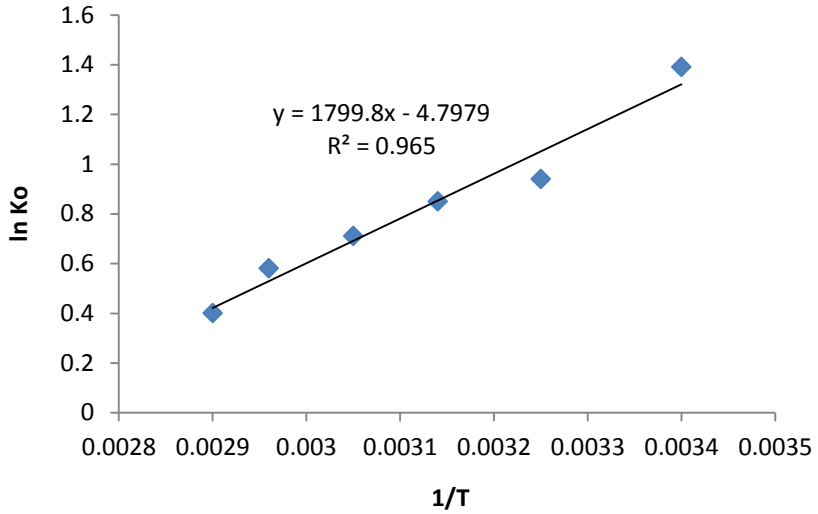

Figure. 12: Plot of ln Kc vs. 1/T for the estimation of thermodynamic parameters.

Table 5: The thermodynamic parameters for the adsorption of (MO) dye onto *Ricinus Communis*-capeed Fe_3O_4NPs. [(MO) dye = 50.0 mgL^{-1}; pH =5.0; dosage sorbent = 0.3 g; time = 60.0 min; stirring speed = 180 rpm]

Dye concn. (mg/L)	ΔH^o(J/mol)	ΔS^o(J/mol K)	ΔG^o(J/mol)		
			300.15K	313.15K	353.15K
(MO) 50(mg/L)	-80.86	-250.517	-6755.5	-452.016	-1723.966

4. CONCLUSION

The selection of *Ricinus Communis*-capeed Fe_3O_4NPs as an efficacious adsorbent for the deletion of (MO) dye from aqueous solutions has been scrutinized. In this current article, the applicability of *Ricinus Communis*-capeed Fe_3O_4NPs as an available, useful, and affordable material for deleting (MO) dye from aqueous media has been confirmed. The desired values of the pH, adsorbent dosage, (MO) dye concentration, and contact time were found to be 5, 0.3 g, 50 mg/L, and 60 min for adsorption of (MO) dye into *Ricinus Communis*-capeed Fe_3O_4NPs. Studying the impact of various process parameters revealed that when initial (MO) dye concentration increased, percent adsorption decreased but percent adsorption enhanced when adsorbent dosage enhanced. The highest (MO) dye deletion by the adsorbent occurred at pH 5.0. The maximum adsorption capacities (q_{max}) were found to be (30.5 mgg^{-1}) for (MO) dye into *Ricinus Communis*-capeed Fe_3O_4NPs respectively. Equilibrium adsorption showed that system followed Langmuir model. The kinetics scrutiny decided that (MO) dye deletion comply with pseudo second-order rate equation. In addition the likelihood of recycling the adsorbent was well proved by desorption studies. Based on the results from the linear regression-based analysis, it was revealed that the derived empirical models represented a passable prediction of performance into *Ricinus Communis*-capeed Fe_3O_4NPs with significant

determination coefficients (R^2= 0.994-0.984). Additionally, the statistical outcomes guaranteed that the recommended equations could favorably be employed for the adsorption of (MO) dye from aqueous solutions. Further investigations on the suitability of this adsorbent for the deletion of other materials have been suggested. Also it was suggested to make inquiries about the suitability of this adsorbent in industrial application. The findings proved the appropriateness of the present procedure for the successful deletion of Pollutants from aqueous solution.

ACKNOWLEDGEMENT

We would like to acknowledge our profound gratitude to the Islamic Azad University, Branch of Omidiyeh, Iran for their partial support of this work.

References:

[1] F. Marahel, Adsorption of Hazardous Methylene Green Dye from Aqueous Solution onto Tin Sulfide Nanoparticles Loaded Activated Carbon: Isotherm and Kinetics Study. Iran. J. Chem. Chem. Eng. 38(5) 129-142 (2019).

[2] A. R. Parvizi, B. Bagheri, N. Karachi, L. Niknam, Preparation and characterization of Titanium dioxide nanoparticles for the Removal of Disulfine Blue and Methyl Orange: spectrophotometric detection and optimization. Orient. J. Chem. 32 (2017) 549-565.

[3] S. A. Haji Azaman, A. Afandi, B. H. Hameed, A.T. Mohd Din, Removal of Malachite Green from Aqueous Phase Using Coconut Shell Activated Carbon: Adsorption, Desorption, and Reusability Studies. J. Appl. Sci. Eng. 21(3) (2018) 317-330.

[4] Gh. Absalan, A. Bananejad, M. Ghasemi, Removal of Alizarin Red and Purpurin from Aqueous Solutions Using Fe_3O_4 Magnetic Nanoparticles. Anal. Bioanal. Chem. Res. 4 (2017) 65-77.

[5] S. Bagheri, Application of response surface methodologhy to modeling and optimization of removal of Bismark Brown and Thymol Blue by Mn-Fe_2O_4-NPs-AC kinetic and thermodynamic studies. Orient. J. Chem. 32 (2016) 549-565.

[6] S. Javad, H. Aghaie, M. Ghaedi, The synthesis of Ag nanoparticles and loading in on activated carbon as a novel adsorbent for removing methyl orange by using surface response methodology. Orient. J. Chem. 30(4) (2014) 1883-1895.

[7] M. A. Salam, S. A. Kosa, A. A. Al-Beladi, Application of nanoclay for the adsorptive removal of Orange G dye from aqueous solution. J. Mol. Liquid. 241 (2017) 469-477.

[8] Z. Zubair, I. Ihsanullah, N. Jarrah, A. Khalid, M. S. Manzar, T. S. Kazeem, M.A. Al- Harthi, Starch-NiFe-layered double hydroxide composites: efficient removal of methyl orange from aqueous phase. J. Mol. Liquids. 249 (2018) 254-264.

[9] J. H. Park, J. J. Wang, R. Xiao, R. D. DeLaune, D. C. Seo, Degradation of Orange G by Fenton-like reaction with Fe-impregnated biochar catalyst. Bioresource. Technol. 249 (2018) 368-376.

[10] A. Reghioua, D. Barkat, A. H. Jawad, A. S. Abdulhameed, A. A. Al-Kahtani, A. A. Al-Othman, Parametric optimization by Box–Behnken design for synthesis of magnetic chitosan-benzil/ZnO/Fe_3O_4 nanocomposite and textile dye removal. J. Environ. Chem. Eng. 9 (2021) 105166.

[11] M. Ishaq, K. Saeed, I. Ahmad, S. Sultan, S. Akhtar, Coal Ash as a Low Cost Adsorbent for the Removal of

Xylenol Orange from Aqueous Solution. Iran. J. Chem. Chem. Eng. 33 (2014) 53-58.

[12] S. Bagheri, H. Aghaei, M. Ghaedi, M. Monajjemi, K. Zare, Novel Au–Fe_3O_4 NPs Loaded on Activated Carbon as a Green and High Efficient Adsorbent for Removal of Dyes from Aqueous Solutions: Application of Ultrasound Wave and Optimization. Eur. J. Anal. Chem. 13(3) (2018) 1-10.

[13] A. M. Vargas, A.C. Martins, V.C. Almeida, Ternary adsorption of acid dyes onto activated carbon from flamboyant pods (Delonix regia): analysis by derivative spectrophotometry and response surface methodology. Chem. Eng. J. 195 (2012) 173-179.

[14] T. M. Coelho, E. Vidotti, M. Rollemberg, A. Medina, M. Baesso, N. Cella, A. Bento, Photoacoustic spectroscopy as a tool for determination of food dyes: comparison with first derivative spectrophotometry. Talanta. 81 (2010) 202-207.

[15] G. Kiani, M. Dostalia, A. Rostami, A.R. Khataee, Adsorption studies on the removal of Malachite Green from aqueous solutions onto halloysite Nanotubes. J. Appl. Clay Sci. 54 (2011) 34-39.

[16] Sh. Davoudi, Adsorption of Methylene blue (MB) dye Using NiO-SiO_2NPs Synthesized from Aqueous Solutions: Optimization, kinetic and equilibrium studies. Iran. J. Chem. Chem. Eng. 40(5) (2021) 1-12.

[17] A. Reghioua, D. Barkat, A.H. Jawad, A.S. Abdulhameed, M.R. Khan, Synthesis of Schiff's base magnetic crosslinked chitosan-glyoxal/ZnO/Fe_3O_4 nanoparticles for enhanced adsorption of organic dye: Modeling and mechanism study. J. Sustaina. Chem. Pharm. 20 (2021) 100379.

[18] S. H. Ahmadi, P. Davar, A. Manbohi, Adsorptive Removal of Reactive Orange 122 from Aqueous Solutions by Ionic Liquid Coated Fe_3O_4 Magnetic Nanoparticles as an Efficient Adsorbent. Iran. J. Chem. Chem. Eng. 35 (2016) 63-73.

[19] F. Marahel, B. Mombeni Goodajdar, N. Basri, L. Niknam, A. A. Ghazali, Applying Neural Network Model for Adsorption Methyl Paraben (MP) dye Using *Ricinus Communis*-capeed Fe_3O_4NPs Synthesized from Aqueous Solution. Iran. J. Chem. Chem. Eng. 40(5) (2021) 1-18.

[20] R. Manohar, V. S. Shrivastava, Adsorption removal of carcinogenic acid violet19 dye from aqueous solution by polyaniline-Fe_2O_3 magnetic nano-composite. J. Mater. Environ. Sci. 6 (2015) 11-21.

[21] G. H. Vatan khah, A. Kohmareh, Enhanced removal of Bismark Brown (BB) dye from aqueous solutions using activated carbon from raw maize tassel: Equilibrium, thermodynamic and kinetics. J. Phys. Theore. Chem. 14(3) (2018) 237-249.

[22] K. Mandel, F. Hutter, C. Gellermann, G. Sextl, Synthesis and Stabilisation of Superparamagnetic Iron Oxide Nanoparticle Dispersions. Colloid. Surf. A: Physicochem. Eng. Aspect. 390 (2011) 173-178.

[23] B. Zargar, H. Parham, A. Hatamie, Fast Removal and Recovery of Amaranth by Modified Iron Oxide Magnetic Nanoparticles. Chemosphere. 76 (2009) 554-557.

[24] A. H. Lu, F. Schuth, Magnetic Nanoparticles: Synthesis, Protection, Functionalization, and Application. Angewand. Chem. Int. Edition. 46 (2007) 1222-1244.

[25] M. Naushad, G. Sharma Zeid, A. Alothman, Photodegradation of toxic dye using Gum Arabic-crosslinkedpoly (acrylamide)/Ni(OH)$_2$/FeOOH nanocomposites hydrogel. J. Clean. Production. 241 (2019) 112863.

[26] A. Dehghanpoor Frashah, S. Hashemian, F. Tamadon, Ag Doped Hydroxyapatite Nano Particles for Removal of Methyl Red Azo Dye from Aqueous Solutions Kinetic and Thermodynamic Studies. Eur. J. Anal. Chem. 15 (2020) 32-44.

[27] F. Maghami, M. Abrishamkar, B. Mombeni Goodajdar, M. Hossieni, Simultaneous adsorption of methylparaben and propylparaben dyes from aqueous solution using synthesized *Albizia lebbeck* leaves-capped silver nanoparticles. Desal. Water Treat. 223 (2021) 388-392.

[28] M. Ghaedi, S. Hajati, B. Barazesh, F. Karimi, G. Ghezelbash, Saccharomyces cerevisiae for the biosorption of basic dyes from binary component systems and the high order derivative spectrophotometric method for simultaneous analysis of Brilliant green and Methylene blue. J. Ind. Eng. Chem. 19 (2013) 227-233.

[29] Sh. Bouroumand, F. Marahel, F. Khazali, Removal of Yellow HE4G dye from Aqueous Solutions Using synthesized Mn-doped PbS (PbS:Mn) nanoparticles. Desal. Water Treat. 223 (2021) 388-392.

[30] W. P. Utomo, E. Santoso, G. Yuhaneka, A. I. Triantini, M. R. Fatqi, M. F. Hudadan, N. Nurfitria, Studi Adsorpsi zat warna Naphthpl Yellow S pada limbah cair Menggunakan aktif dari ampas tebu. Journal Kimia (Journal of chemistry). 13 (2019) 104-116**.**

[31] M. Ghaemi, G. Absalan, L. Sheikhian, Adsorption characteristics of Titan yellow and Congo red on $CoFe_2O_4$ magnetic nanoparticles. J. Iran. Chem. Soc. 11 (2014) 1759-1766.

[32] S. Shariati, M. Faraji, Y. Yamini, A. A. Rajabi, Fe_3O_4 Magnetic Nanoparticles Modified with Sodium Dodecyl Sulfate for Removal of Safranin O Dye from Aqueous Solutions. Desalination. 270 (2011) 160-165.

[33] M. Ghaedi, B. Sadeghian, A. A. Pebdani, R. Sahraei, A. Daneshfar, C. Duran, Kinetics, thermodynamics and equilibrium evaluation of direct yellow 12 removal by adsorption onto silver nanoparticles loaded activated carbon. Chem. Eng. J. 187 (2012) 133–141.

[34] A. Achmad, J. Kassim, T. Kim Suan, Equilibrium, Kinetic and Thermodynamic Studies on the Adsorption of Direct Dye onto a Novel Green Adsorbent Developed from Uncaria Gambir Extract. J. Phys. Sci. 23 (2012) 1-13.

[35] R. Mahini, H. Esmaeili, R. Foroutan, Adsorption of methyl violet from aqueous solution using brown algae Padina sanctae-crucis. Turk. J. Biochem. 24 (2018) 1-12.

[36] S. Hajati, M. Ghaedi, H. Mazaheri, Removal of methylene blue from aqueous solution by walnut carbon: optimization using response surface methodology. Desal. Water Treat. 57 (2016) 3179-3193.

[37] S. Hajati, M. Ghaedi, B. Barazesh, F. Karimi, R. Sahraei, A. Daneshfar, A. Asghari, Application of high order derivative spectrophotometry to resolve the spectra overlap between BG and MB for the simultaneous determination of them: ruthenium nanoparticle loaded activated carbon as adsorbent. J. Ind. Eng. Chem. 20 (2014) 2421-2427.

[38] Y. Yang, Y. Xie, L. Pang, M. Li, X. Song, J. Wen, H. Zhao, Preparation of reduced graphene oxide/poly(acrylamide) nanocomposite and its adsorption of Pb^{2+} and methylene blue. Langmuir. 29 (2013) 10727-10736.

[39] A.A. Ghazali, Ultrasonic Assisted Removal of Methyl Paraben (MP) on Ultrasonically Synthesized $Zn(OH)_2$-NPs-AC: Experimental Design Methodology. J. Phys. Theore. Chem. 19(1) (2021) 65-78.

[40] C. Arora, S. Soni, S. Sahu, J. Mittal, P. Kumar, P.K. Bajpai, Iron based metal organic framework for efficient removal of methylene blue dye from industrial waste. J. Mol. Liquids. 284 (2019) 373-352.

[41] E. Mousavi, A. Geramizadegan, Adsorption of Benzyl Paraben Dye from Aqueous Solutions Using synthesized Mn-doped PbS (PbS:Mn) nanoparticles. J. Phys. Theore. Chem. 17(3,4) (2020) 123-143.

[42] G. H. Haghdoost, Removal of Reactive Red 120 from Aqueous Solutions Using Albizia lebbeck Fruit (Pod) Partical as a Low Cost Adsorbent. J. Phys. Theore. Chem. 15(3,4) (2019) 141-148.

[43] M. Hubbe, S. Azizian, S. Douven, Implications of Apparent Pseudo-Secound-Order Adsorption Kinetics onto Cellulosic Materials: A Review. Bio Resources. 14(3) (2019) 7582-7626.

[44] M. Toor and B. Jin, Adsorption Characteristics, Isotherm, Kinetics, and Diffusion of Modified Natural Bentonite for Removing Diazo Dye. Chem. Eng. J. 187 (2012) 79-88.

[45] F. Bouaziz, M. Koubaa, F. Kallel, R. E. Ghorbel, S.E. Chaabouni, Adsorptive Removal of Malachite Green from Aqueous Solutions by Almond Gum: Kinetic Study and Equilibrium Isotherms. Int. J. Biol. Macromolecule. 105 (2017) 56-65.

[46] H. S. Ghazi Mokri, N. Modirshahla, M.A. Behnajady, B. Vahid, Adsorption of C.I. Acid Red 97 dye from aqueous solution onto walnut shell: kinetics, thermodynamics parameters, isotherms. Int. J. Environ. Sci. Technol. 12 (2015) 1401–1408.

[47] S. Banerjee, G. C. Sharma, P. K. Gautam, M. C. Chatto padhyaya, S. N. Upadhyay, Y.C. Sharma, Removal of Malachite Green, a Hazardous Dye from Aqueous Solutions Using Avena Sativa (oat) Hull as a Potential Adsorbent. J. Mol. Liquid. 213 (2016) 162-172.

مجله شیمی فیزیک و شیمی نظری
دانشگاه آزاد اسلامی واحد علوم و تحقیقات
جلد ۱۸، شماره ۳، پاییز ۱۴۰۰
ISSN ۱۷۳۵-۲۱۲۶

مطالعات حذف رنگ متیل اورانژ با استفاده از جاذب برگ کرچک اصلاح شده با نانوذران اکسید آهن از محلول‌های آبی

لیلا نیکنام* و شهناز داوودی

گروه شیمی واحد امیدیه، دانشگاه آزاد اسلامی، امیدیه، ایران

چکیده

کاربرد برگ گیاه کرچک اصلاح شده با نانوذرات اکسید آهن سنتزی برای حذف رنگ‌ها از محیط‌های آبی تایید شده است. تکنیک‌های یکسانی از جملهFT-IR ، BET، XRDو SEM برای توصیف این ماده جدید استفاده شده است. و بررسی قابلیت کاربرد برگ کرچک اصلاح شده با نانوذرات اکسید آهن را به عنوان یک جاذب در دسترس، مناسب و کم هزینه برای حذف مناسب رنگ متیل اورنج (MO) از محیط‌های آبی نشان داد. مقدارpH 5.0 ، دوز جاذب ۰,۳ گرم، غلظت رنگ متیل اورانژ ۵۰ میلی گرم در لیتر، و زمان تماس ٦۰ دقیقه مقادیر بهینه جذب روی برگ کرچک اصلاح شده با نانوذرات اکسید آهن در نظر گرفته شده است. بررسی تأثیر پارامترهای مختلف نشان داد که درصد جذب و غلظت اولیه رنگ متیل اورانژ رابطه معکوس دارند در حالی که درصد جذب و دوز جاذب رابطه مستقیم دارند. نشان داده شد که حذف رنگ متیل اورانژ توسط جاذب، ایزوترم همدمای لانگمویر در توصیف داده‌های تعادلی بهتر از سایر مدل‌ها در pH 5.0 بود. پارامترهای ترمودینامیکی انرژی آزاد (ΔG^0) ، آنتالپی (ΔH^0) و آنتروپی (ΔS^0) جذب با استفاده از ایزوترم تعیین شد. این واقعیت که فرآیند جذب گرمازا بود به خوبی با مقدار منفیΔG^o ، ΔH^oو ΔS^o منعکس شد که به خودی خود تمایل برگ کرچک اصلاح شده با نانوذرات اکسید آهن را برای حذف رنگ متیل اورانژ بیان می‌کند. حداکثر ظرفیت جذب برای رنگ متیل اورانژ در شرایط مطلوب (۳۰,۵ میلی گرم در گرم) مشاهده شد.

کلید واژه‌ها: رنگ متیل اورانژ، ظرفیت جذب، ایزوترم لانگمویر، ترمودینامیک

* مسئول مکاتبات: leila.niknam352@gmail.com